

# Submicron x-ray diffraction and its applications to problems in materials and environmental science

N. Tamura,<sup>a)</sup> R. S. Celestre, A. A. MacDowell, and H. A. Padmore

*ALS/Lawrence Berkeley National Laboratory, 1 Cyclotron Road, Berkeley, California 94720*

R. Spolenak

*Agere Systems, formerly of Bell Labs, Lucent Technologies, Murray Hill, New Jersey 07974*

B. C. Valek and N. Meier Chang

*Department of Materials Science and Engineering, Stanford University, Stanford, California 94305*

A. Manceau

*Environmental Geochemistry Group, LGIT, University J. Fourier, 38041 Grenoble Cedex 9, France*

J. R. Patel

*ALS/Lawrence Berkeley National Laboratory, 1 Cyclotron Road, Berkeley, California 94720 and SSRL/SLAC, Stanford University, Stanford, California 94309*

(Presented on 22 August 2001)

The availability of high brilliance third generation synchrotron sources together with progress in achromatic focusing optics allows us to add submicron spatial resolution to the conventional century-old x-ray diffraction technique. The new capabilities include the possibility to map *in situ*, grain orientations, crystalline phase distribution, and full strain/stress tensors at a very local level, by combining white and monochromatic x-ray microbeam diffraction. This is particularly relevant for high technology industry where the understanding of material properties at a microstructural level becomes increasingly important. After describing the latest advances in the submicron x-ray diffraction techniques at the Advanced Light Source, we will give some examples of its application in material science for the measurement of strain/stress in metallic thin films and interconnects. Its use in the field of environmental science will also be discussed. © 2002 American Institute of Physics. [DOI: 10.1063/1.1436539]

## I. INTRODUCTION

Materials properties such as strength, resistance to fatigue, and failure intimately depend on their microstructural features such as grains, grain boundaries, inclusions, voids, and other defects. However, at the so-called mesoscopic length scale (approximately between 0.1 and 10  $\mu\text{m}$ ) polycrystalline materials typically exhibit high inhomogeneity, and properties are extremely difficult to study both experimentally and theoretically. This length scale is situated between the atomic scale of atoms and individual dislocations, and the macroscopic scale of continuum mechanics.

X-ray diffraction is a powerful technique, used for almost a century to measure grain orientation and strain, as well as for crystalline phase identification and structure refinement. Compared to electron microscopy, x rays have the advantages of higher penetration depth (rendering possible the scanning of bulk and buried samples), do not require any particular sample preparation, and can be used under a variety of different conditions (in air, liquid, vacuum or gas, at different temperature and pressures). Its main drawback for the study of materials at the micron scale was until recently its poor spatial resolution.

Today, the availability of high brilliance third generation synchrotron sources, combined with progress in x-ray focus-

ing optics and fast two-dimensional large area detector technology have made possible the development of scanning x-ray microdiffraction ( $\mu\text{SXR}$ ) techniques using either monochromatic or polychromatic focused beams of sizes ranging from a few microns to submicron.<sup>1-8</sup> The closest equivalents in the electron microscopy field are scanning transmission electron microscopy and electron backscatter diffraction. The spatial resolution of electron microscopy is still about an order of magnitude better than focused x rays, but the two techniques are complementary, with x-ray microdiffraction being a superior technique for looking at subsurface structures, and for precision measurements of stress.

Recently, an x-ray microdiffraction end station capable of measuring grain orientation and triaxial strain in arbitrarily oriented micron-sized crystals has become available at the Advanced Light Source (ALS) on beamline 7.3.3. This article describes practical applications provided by this tool.

## II. BEAMLINE DESCRIPTION

The experimental setting of the 7.3.3. beamline end station is shown in Fig. 1 and has been described in details elsewhere.<sup>8</sup> The x-ray synchrotron beam from a bending magnet source is focused via a pair of bendable Kirkpatrick-Baez mirrors to a submicron size ( $0.7 \times 0.8 \mu\text{m}$  full width at half maximum). A four-crystal Si(111) monochromator is used to easily switch between white and monochromatic beams while the same area on the sample is illuminated. The

<sup>a)</sup>Author to whom correspondence should be addressed; electronic mail: ntamura@lbl.gov

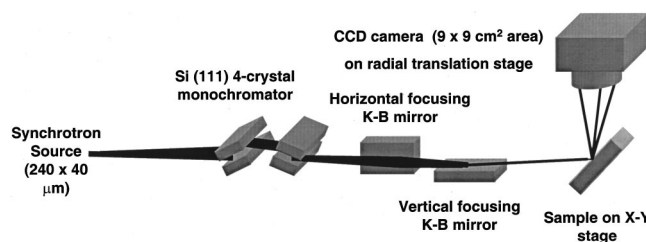


FIG. 1. Schematic layout of the micro-diffraction end station on beamline 7.3.3. at the ALS.

sample is usually in the reflective geometry arrangement, the surface making an angle of  $45^\circ$  relatively to the incoming beam. The outgoing Bragg reflections are collected using a large area charge coupled device detector (Bruker 6000, active area of  $9 \times 9$  cm) placed  $\sim 3$  cm above the sample. For single crystals and polycrystalline samples with grain size on the order of 1 micron, the so-called white beam or Laue reflection technique is used. Illuminating an area of interest with submicron white beam provides a Laue pattern which can be image treated and automatically indexed. The indexing yields at the same time the crystal orientation and deviatoric (distortional) strain tensor of the illuminated area. By putting the sample on an  $X$ - $Y$  piezo stage, it can be scanned under the focused beam with submicron step size. This allows orientation and strain/stress mapping of the material. The complete strain tensor (six components) can also be computed by additionally determining the dilational (“hydrostatic”) component. This can be achieved by measuring the energy of at least one reflection using the monochromator.<sup>1,2,4</sup> For finely grained samples, monochromatic beam is preferentially used and a powder ring pattern is collected at each step of the  $X$ - $Y$  scan. A solid state detector coupled with a multichannel analyzer allows for the parallel collection of fluorescence signals which allows for elemental mapping. A software package developed at the

ALS (X-MAS for X-Ray Microdiffraction Analysis Software) is used for data collection, Laue pattern indexing, strain refinement, and monochromatic beam scans analysis. For polycrystals, an orientation map “smoothing” algorithm also allows for the automatic determination of grain boundaries by fitting the intensity profile of each individual crystal grain and intersecting the resulting normalized profiles.

### III. APPLICATIONS

#### A. Thermal stress measurements in Al(Cu) interconnect

The samples consist of patterned Al(0.5% wt. Cu) lines (length:  $30 \mu\text{m}$ , thickness:  $0.7 \mu\text{m}$ , width:  $4.1$  and  $0.7 \mu\text{m}$ ) sputter deposited on a Si wafer and buried under a glass passivation layer ( $0.7 \mu\text{m}$  thick). As a comparison, data have also been taken on unpassivated Al(Cu) pads (blanket films).

Figure 2 shows orientation and deviatoric stress maps on a  $5 \times 5 \mu\text{m}$  region in the pad and on the  $4.1$  and  $0.7 \mu\text{m}$  wide lines. The stress in the pad appears to be biaxially tensile in average, which is consistent with macroscopic stress measurements using wafer curvature and conventional x-ray diffraction techniques. However, at a microscopic scale, stress is actually far from being homogeneous. It is triaxial rather than biaxial, with local differences reaching  $60$ – $80$  MPa.

Similarly, lines displayed local variations of  $60$ – $80$  MPa in stress for the  $4.1 \mu\text{m}$  line and up to  $140$  MPa for the  $0.7 \mu\text{m}$  line. As the line gets narrower, the level of stress gets higher and, on average, shifts from biaxial to triaxial. Orientation maps also show the change in the microstructure from polycrystalline in the pad and in the  $4.1 \mu\text{m}$  line to “bamboo” type for the  $0.7 \mu\text{m}$  line. Temperature cycling experiments between  $25$  and  $345^\circ\text{C}$  have been carried out on these same lines<sup>9</sup> and show good agreement of the average stress–temperature curves with those obtained with conventional techniques, but show a high degree of complexity on the

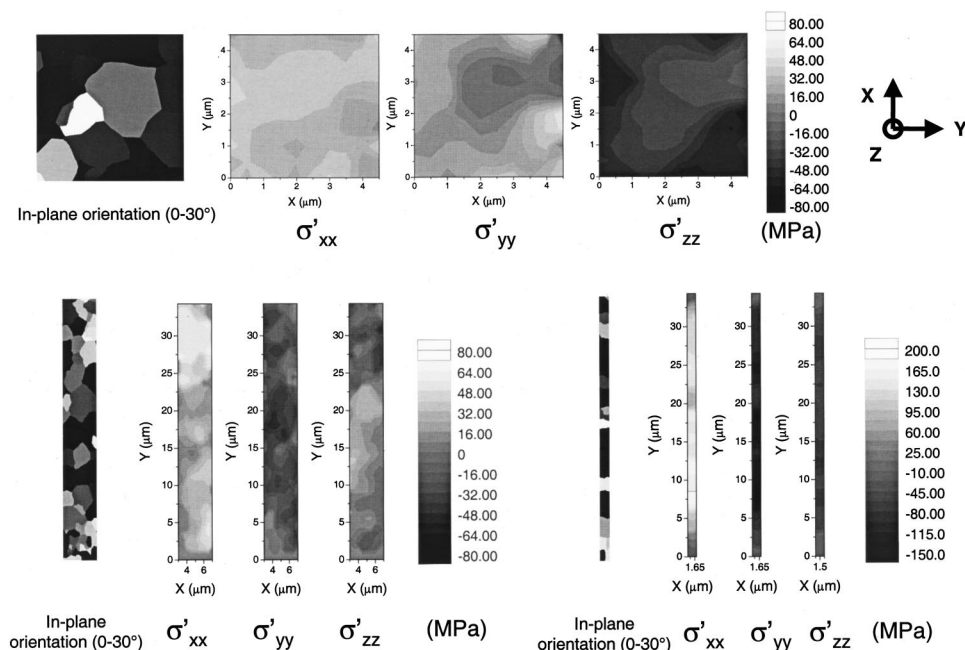


FIG. 2. In-plane orientation and deviatoric stress components along  $x$ ,  $y$ , and  $z$  for the Al(Cu) unpassivated blanket film (top),  $4.1 \mu\text{m}$  wide passivated line (bottom left) and  $0.7 \mu\text{m}$  wide passivated line (bottom right).

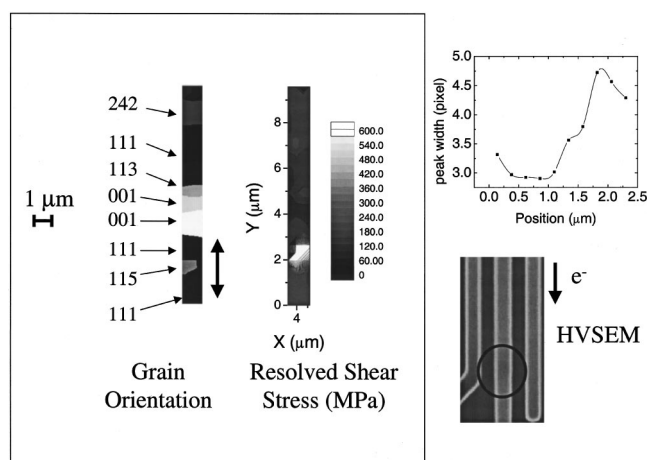


FIG. 3. Grain orientation and resolved shear stress maps obtained by the scanning x-ray microdiffraction Laue technique. The HVSEM image (bottom right) shows a region of metal accumulation.

local scale. Large intergranular and intragranular stress variations have been measured indicating that local parameters such as grain orientation, grain initial stress, grain size, and type of grain boundaries play a crucial role in understanding the inhomogeneous yielding mechanisms of polycrystalline thin films. This particular example shows the ability of x-ray microdiffraction to provide quantitative data such as grain orientation, structure, and stress at the local level in passivated interconnects, greatly improving the understanding and modeling of material mechanical properties under constraints.

### B. Electromigration in damascene Cu interconnects

Figure 3 shows a region of a sputtered copper damascene interconnect (1.1  $\mu\text{m}$  wide, passivated with nitride) that has undergone electromigration testing.<sup>10</sup> The bottom right inset shows a high voltage scanning electron microscope (HVSEM) image taken just after the electromigration test, near the cathode end. The metal buildup region (marked by a black circle) appears as a slightly darker zone in the electromigrated line. The corresponding orientation and resolved shear stress (calculated from the measured distortional stresses and considering the 12 glide systems of Cu: (111) type planes in the  $\langle 110 \rangle$  directions) maps obtained by  $\mu\text{SXRD}$  are displayed on the left. The grain structure has a random out-of-plane orientation and a near-bamboo structure. The indices, next to the map, indicate the approximate out-of-plane orientation of the largest grains. At the location of the local buildup region, the resolved shear stress dramatically increases to reach a maximum value of about 600 MPa. The orientation map shows that metal has accumulated at the interface of a (111) bamboo grain just before the location of a (115) twin and after a series of small randomly oriented grains (the latter will allow for a fast electromigration diffusion path). The width of the Bragg reflections also contains information on the dislocation density and provides an indication on the level of stress and plastic deformation inside a particular grain. The peak width of the (113) reflection is plotted (top right) as a function of the position along the 2  $\mu\text{m}$  long (111) grain (indicated by the black double-sided

arrow next to the orientation map), which contains the (115) blocking twin. The peak is clearly broader in the buildup region next to the twin boundary.

Electromigration-induced failure in interconnect metal lines are highly dependant on the microstructure and initial stress states of the samples. The capability demonstrated by the instrument to nondestructively probe local grain structure as well as stress becomes particularly relevant to the understanding of microstructure-related failure mechanisms and to predict where the line is likely to fail during service. This technologically important problem is shown to be much more complex when the line dimensions shrink to a size where microstructural local effects could no longer be neglected.

### C. Element speciation in soil micronodules

Soils are chemically and structurally highly heterogeneous, rendering the identification of finely dispersed mineral species difficult, if at all possible, with conventional laboratory diffractometers. Since environmental materials are heterogeneous on nanometer to micrometer length scales, the combination of synchrotron-based x-ray radiation microfluorescence ( $\mu\text{SXRF}$ ) and  $\mu\text{XRD}$  techniques provides just the tool needed to make the key identification of most reactive constituents, and the uptake mechanism of associated trace elements. These new scientific opportunities will be illustrated by the sequestration mechanism of Zn and Ni in soils. Figure 4(a) shows Mn, Fe, Zn, and Ni chemical maps as determined by  $\mu\text{SXRF}$ . Zn and Ni are both associated with Mn but unlike Zn, Ni is not present in the entire Mn region, suggesting the presence of at least two distinct Mn species. A phyllosilicate component, an Fe oxyhydroxide, goethite ( $\alpha\text{FeOOH}$ ), and two Mn oxides (birnessite and lithiophorite), were positively identified by  $\mu\text{XRD}$  [Fig. 4(b)]. The lithiophorite structure consists of mixed  $\text{MnO}_2$  layer structure in which Mn atoms are adsorbed in the interlayer space above and below vacant layer octahedral sites [Fig. 4(c)].<sup>11</sup> The soil sample was scanned with a 6 keV monochromatic beam, and a diffraction pattern was collected at each step. The automated analysis of the powder ring patterns yielded the mineral species distribution maps presented in Fig. 4(d). The comparison of chemical and mineral species maps indicate that Ni is exclusively associated with the lithiophorite, whereas Zn is partitioned between lithiophorite, birnessite and phyllosilicates (not shown). In future studies, the crystallographic sites of Ni and Zn in their host phases will be determined by extended x-ray absorption fine structure ( $\mu\text{EXAFS}$ ).<sup>12</sup> The combination of these three micron-scale techniques is unprecedented and is quite powerful in advancing the scientific state-of-the-art for the remediation of contaminated sites.

### IV. CONCLUSION

Scanning x-ray microdiffusion using white and/or monochromatic beams offer a powerful tool to study material properties at the micron scale. The white beam technique is suitable for *in situ* study of microtexture and strain in single crystal and polycrystalline thin films. It was applied to study



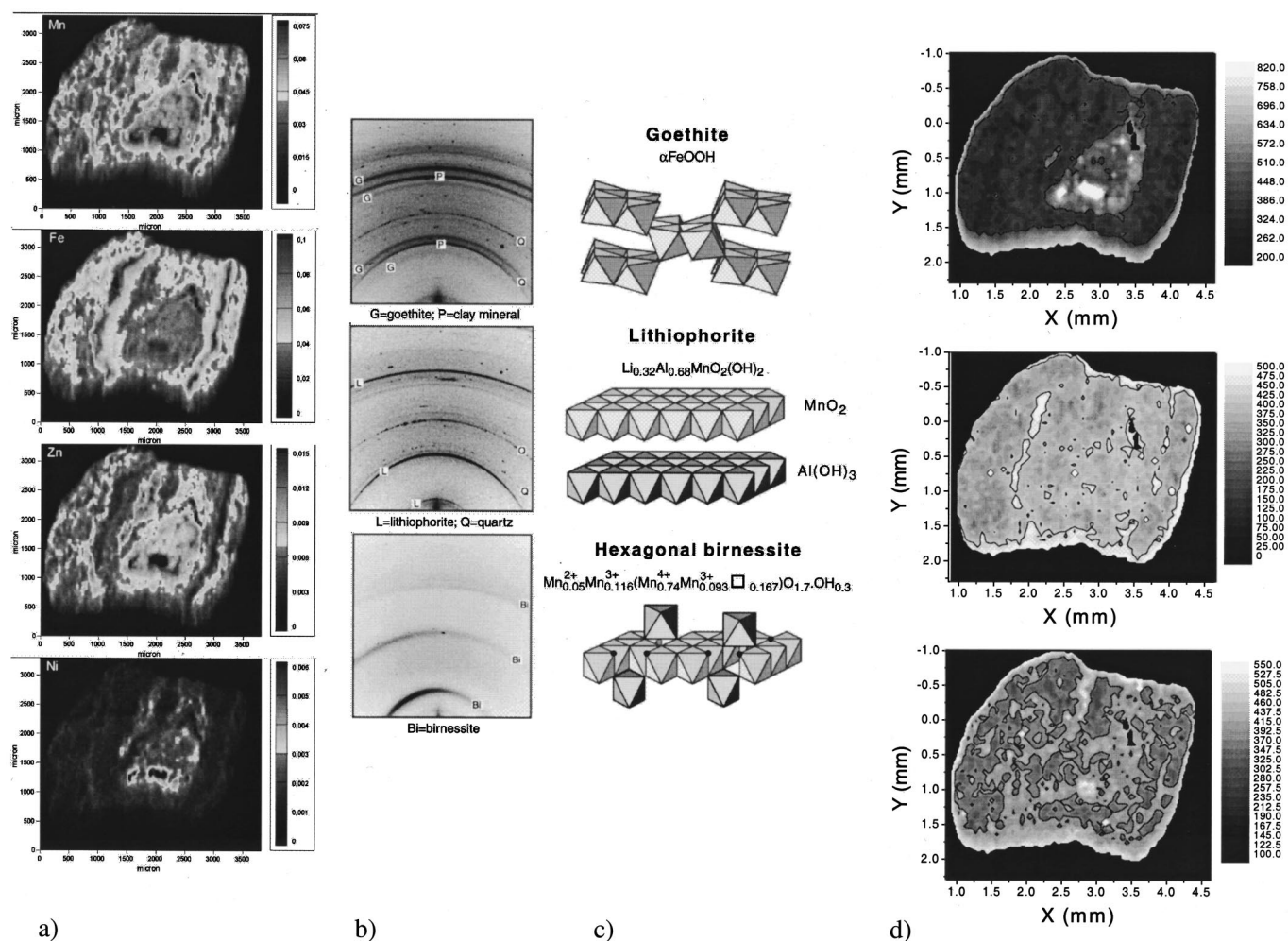


FIG. 4. (a) Mn, Fe, Zn, and Ni chemical maps of a soil micronodule obtained by  $\mu\text{XRF}$ . (b) Microdiffraction patterns in selected regions in the map. (c) Crystallographic structures of goethite, lithiophorite, and hexagonal birnessite. (d) Mineral species distribution maps (top to bottom) for lithiophorite, goethite, and hexagonal birnessite obtained by monochromatic  $\mu\text{SXRD}$ .

electromigration damage in microchip interconnects, as well as studying the effect of confinement during thermal cycles. The applicability of the technique was also recently demonstrated in the study of deformation in microelectromechanical systems (MEMS) devices, composite materials, and *in situ* uniaxial tensile testing of polycrystalline samples and will be addressed in forthcoming articles. Monochromatic  $\mu\text{SXRD}$ , coupled with  $\mu\text{SXRF}$  and  $\mu\text{EXAFS}$ , is a new and promising technique, which should have a significant impact on molecular environmental science.<sup>13</sup> Future work includes the use of monochromatic  $\mu\text{SXRD}$  for strain mapping in thin metallic films subject to spontaneous debonding from the substrate and metallic membranes under uniaxial tensile strain.

## ACKNOWLEDGMENTS

The Advanced Light Source is supported by the Director, Office of Science, Office of Basic Energy Sciences, Materials Sciences Division, of the U.S. Department of Energy under Contract No. DE-AC03-76SF0098 at Lawrence Berkeley

National Laboratory. The authors thank Intel Corp. for the partial funding of the end station.

- <sup>1</sup>J. S. Chung, N. Tamura, G. E. Ice, B. C. Larson, J. D. Budai, and W. Lowe, *Mater. Res. Soc. Symp. Proc.* **563**, 169 (1999).
- <sup>2</sup>N. Tamura, J.-S. Chung, G. E. Ice, B. C. Larson, J. D. Budai, J. Z. Tischler, M. Yoon, E. L. Williams, and W. P. Lowe, *Mater. Res. Soc. Symp. Proc.* **563**, 175 (1999).
- <sup>3</sup>B. C. Larson, N. Tamura, J.-S. Chung, G. E. Ice, J. D. Budai, J. Z. Tischler, W. Yang, H. Weiland, and W. P. Lowe, *Mater. Res. Soc. Symp. Proc.* **590**, 247 (2000).
- <sup>4</sup>N. Tamura *et al.*, *Mater. Res. Soc. Symp. Proc.* **612**, D8.8.1 (2000).
- <sup>5</sup>R. Spolenak *et al.*, *Mater. Res. Soc. Symp. Proc.* **612**, D.10.3.1 (2000).
- <sup>6</sup>C. Riekel, C. Braenden, C. Craig, C. Ferrero, F. Heidelbach, and M. Müller, *Int. J. Mol. Biol.* **24**, 187 (1999).
- <sup>7</sup>C. Riekel, *Rep. Prog. Phys.* **63**, 233 (2000).
- <sup>8</sup>A. A. MacDowell *et al.*, *Nucl. Instrum. Methods Phys. Res. A* **467–468**, 936 (2001).
- <sup>9</sup>B. C. Valek *et al.*, *Mater. Res. Soc. Symp. Proc.* **673**, P7.7 (2001).
- <sup>10</sup>B. C. Valek *et al.* (unpublished).
- <sup>11</sup>B. Lanson, V. A. Drits, E. J. Silvester, and A. Manceau, *Am. Mineral.* **85**, 826 (2000).
- <sup>12</sup>A. Manceau, B. Lanson, M. L. Schlegel, J. C. Hargé, M. Musso, L. Eybert-Bérard, J. L. Hazemann, D. Chateigner, and G. M. Lambie, *Am. J. Sci.* **300**, 289 (2000).
- <sup>13</sup>S. Hlawatsch, M. Kersten, C. D. Garbe-Schönberg, F. Lechtenberg, A. Manceau, N. Tamura, D. A. Kulik, J. Harff, and E. Suess, *Chem. Geol.* (to be published).